Polarization based Microscopy using a Fiber Optic Spectral Polarimeter

Eunha Kim, Digant P Dave, Thomas E. Milner
Department of Biomedical Engineering, The University of Texas at Austin

ABSTRCT

We present a fiber optic spectral polarimeter, an instrument that allows measurement of the spectrally resolved Stokes parameters. The instrument consists of a pair of polarization maintaining (PM) fibers spliced at 45° with respect to each other in line with a polarizer module whose transmission axis is aligned to the fast axis of the first PM fiber. The generated spectrum is composed of three quasi-cosinusoidal components, which carry information required to reconstruct the spectrally resolved Stokes parameters of incident light. Fourier transform of the measured spectrum provides the significant parameters for determination of the spectrally resolved Stokes parameters of light. The performance of the fiber optic spectral polarimeter is demonstrated by the computer simulation and experiments with input light of known polarization states. A unique characteristic of this instrument is that the spectrally resolved polarization state of incident light can be determined from one spectral measurent without any mechanical movement. Moreover, the instrument can be incorporated into a tomographic imaging system such as a conventional microscopy system. Polarization based microscopy combined with a fiber optic spectral polarimeter will provide measurements that allow better understanding of depolarization process of light passing through biological materials for diagnostic imaging.

Keywords: Polarization State of Light, Stokes Parameters, Scattering

1. INTRODUCTION

The polarization state of light scattered by the tissue has been considered to be important as a contrast mechanism in biomedical imaging. Various investigators have suggested that the degree of polarization can be used as a discrimination criterion by which to extract weakly scattered from the multiply scattered light [1-3] and improve the image quality [4, 5]. This method is based on the depolarization effect in random scattering of tissues. Also, measurements of polarization state changes of light backscattered from tissue with low-coherence interferometry were used to estimate birefringence of various tissues such as collagen, muscle fibers, and retina [6-8]. Moreover, since the polarization state changes depend on the geometric and scattering properties of the scatterers, polarization analysis of light scattered from tissue can offer a potential method for probing the tissue [9-11]. However, polarized light studies have been considered not to be applicable to thick tissue samples such as breast or brain since the polarization information is destroyed after relatively few scattering events. Recently, the spectral polarization difference imaging technique was proposed as an imaging tool that can provide subsurface imaging with depth of the order of 1-cm [12].
In the conventional measurement of the polarization state of light using a single detector, polarization-analyzing optics, consisting of a quarter wave plate and polarizer, are used. Unfortunately, the method generally involves mechanical movement of the polarization-analyzing optics followed by several measurements. Therefore measurement of the complete polarization state requires a long time relative to coherence time of the source and may affect the measured polarization state of light. The unique characteristic of the proposed spectral polarimeter is that the spectrally resolved polarization state can be determined from just one spectral measurent without any mechanical movement. And spectral variations of the polarization state of light allow the investigation of the depolarization process of light propagating in tissue. Furthermore, it may enable to develop a unique tomographic imaging technique.

2. BACKGROUND

The representation known as Stokes parameters uses four quantities based on six intensity measurements with different combinations of the polarizer and quarter wave plate, known as Stokes parameters [13].

$$S_0 = I_{0^\circ} + I_{90^\circ} \tag{1.a}$$

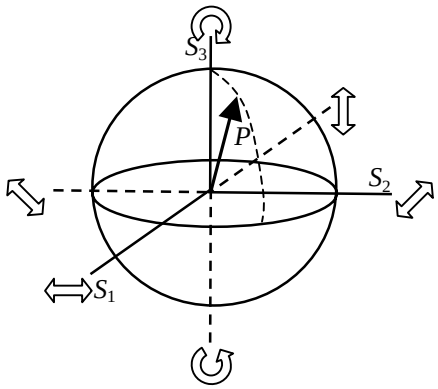

Figure 1. Schematic Illustration of Poincaré Sphere.

$$S_1 = I_{0^\circ} - I_{90^\circ} \tag{1.b}$$

$$S_2 = I_{45^\circ} - I_{-45^\circ} \tag{1.c}$$

$$S_2 = I_{45^\circ,\lambda/4} + I_{-45^\circ,\lambda/4} \tag{1.d}$$

where I_{θ° and $I_{\theta^\circ,\lambda/4}$ are the measured intensities with the linear polarizer at angle θ°, and the polarizer in line with a quarter wave plate in front of the detector respectively. S_0 is simply the total light intensity and S_1, S_2 and S_3 specify the polarization states that represent the portion of the light polarized horizontally, linearly at 45° and circularly, respectively. If the light is horizontally polarized, Stokes parameters normalized by S_0 are (1, 1, 0, 0). Similarly, the Stokes parameters for the vertical linearly polarized light is (1, -1, 0, 0). The degree of polarization of the light is given by

$$P = \frac{\sqrt{S_1^2 + S_2^2 + S_3^2}}{S_0}. \tag{2}$$

For completely polarized light, the degree of polarization is unity and for partially polarized light, $0<P<1$. If two incoherent monochromatic polarized lights described as (S_0', S_1', S_2', S_3') and (S_0'', S_1'', S_2'', S_3'') are superimposed, the resultant light can be expressed as ($S_0'+S_0''$, $S_1'+S_1''$, $S_2'+S_2''$, $S_3'+S_3''$).

One advantage of the Stokes parameter representation is that the polarization of light can be visualized using the Poincaré sphere with a radius of S_0 [14]. In the Poincaré sphere representation shown in Figure 1, the polarization of light is represented as a vector (P) with coordinates (S_1, S_2, S_3). If the light is completely polarized the end point of the vector P is on the sphere surface, otherwise, (S_1, S_2, S_3) is inside the sphere ($S_1^2+S_2^3+S_3^2<S_0^2$). Adding two incoherent light states, the polarization of resultant light is a sum of two polarization vectors. An important result for our analysis later is the polarization state of broadband light can be considered as a sum of Stokes vectors representing each spectral component.

When light propagating in tissue encounters the scatterer, the phase and amplitude of each spectral component of the light are modified by the single scattering event inside the tissue, resulting in the polarization state change, and this scattering effect on the polarization is not perfectly correlated between spectral components. Since the Stokes parameters of the light is a sum of the Stokes parameters of each spectral component, unequal scattering effect on different spectral components produces partial or complete depolarization of scattered light.

3. METHODS

This section presents the principle of a spectral polarimeter-an instrument to quantify the complete polarization state of collected light over a bounded continuum of optical frequencies. The basic scheme of the spectral polarimeter is illustrated in Figure 2 [15]. The light to be measured ($I_{in}(\nu)$) has a broad spectrum and its polarization state changes with

frequency [$S_0(\nu)$, $S_1(\nu)$, $S_2(\nu)$, $S_3(\nu)$]. The spectral polarimeter is composed of a pair of linear retarders (R1 and R2) aligned at 45° with respect to each other and a polarizer (P) whose transmission axis is aligned with respect to the fast axis of R1. Assuming the x and y axes are coincident with the fast and slow axes of R1, orthogonal oscillations of incident light, E_x and E_y, experience a phase delay passing through the first retarder by $2\pi\nu n_f L_1/c$ and $2\pi\nu n_s L_1/c$, respectively, where n_f and n_s are the refractive indices of a retarder along the fast and slow axes, and L_1 is a length of the first retarder. E_x and E_y are then launched into the second retarder and the both oscillations are projected on its fast and slow axes with equal amplitude. The light exiting from the second retarder has four components with different phase delays, $E_x(2\pi\nu n_f L_1/c+2\pi\nu n_f L_2/c)$, $E_x(2\pi\nu n_f L_1/c+2\pi\nu n_s L_2/c)$, $E_y(2\pi\nu n_s L_1/c+2\pi\nu n_f L_2/c)$, and $E_y(2\pi\nu n_s L_1/c+2\pi\nu n_s L_2/c)$ where the quantity in a parenthesis represents the phase delays that each oscillation of the input light experiences by a paired retarder system. A polarizer, P, projects all components of the light on its the transmission axis, P, and produces an interference fringe between each component.

Using Jones vectors representing the light in terms of two orthogonal electric fields at each optical frequency (ν) and Jones matrices for linear optical elements such as the retarder and polarizer [1], light emerging from a spectral polarimeter can be determined:

$$\begin{aligned} I_{out}(\nu) = & \frac{1}{2}S_0(\nu) + \frac{1}{2}S_1(\nu)\cos(\varphi_2(\nu)) \\ & + \frac{1}{4}\left|S_{23}(\nu)\right|\cos\left[(\varphi_1(\nu) - \varphi_2(\nu)) - \arg(S_{23}(\nu))\right] \\ & - \frac{1}{4}\left|S_{23}(\nu)\right|\cos\left[(\varphi_1(\nu) + \varphi_2(\nu)) - \arg(S_{23}(\nu))\right] \end{aligned} \tag{3}$$

with

$$S_{23}(\nu) = S_2(\nu) - iS_3(\nu), \tag{4}$$

where $\varphi_1(\nu)$ and $\varphi_2(\nu)$ are the phase retardations between light that propagate along the fast and slow axes of the R1 and R2, respectively.

$$\varphi_{1,2}(\nu) = \frac{2\pi\nu(n_s - n_f)L_{1,2}}{c} \tag{5}$$

As can be understood from Equation (3), $I_{out}(\nu)$ includes three quasi-cosinusoidal components, which carry the information about spectrally resolved Stokes parameters of incident light onto the spectral polarimeter.

We now consider how to demodulate the Stokes parameters from the obtained $I_{out}(\nu)$. Fourier transform of Equation (3) gives

$$\begin{aligned} \Im[I_{out}(\nu)] = & \frac{1}{2}\Im[S_0(\nu)](x) \\ & + \frac{1}{4}\Im[S_1(\nu)](x - \Delta nL_2) + \frac{1}{4}\Im[S_1(\nu)](x + \Delta nL_2) \\ & + \frac{1}{8}\Im[S_{23}(\nu)](x - \Delta n(L_2 - L_1)) + \frac{1}{8}\Im[S_{23}^*(\nu)](x + \Delta n(L_2 - L_1)) \\ & - \frac{1}{8}\Im[S_{23}(\nu)](x + \Delta n(L_2 + L_1)) - \frac{1}{8}\Im[S_{23}^*(\nu)](x - \Delta n(L_2 + L_1)) \end{aligned} \tag{6}$$

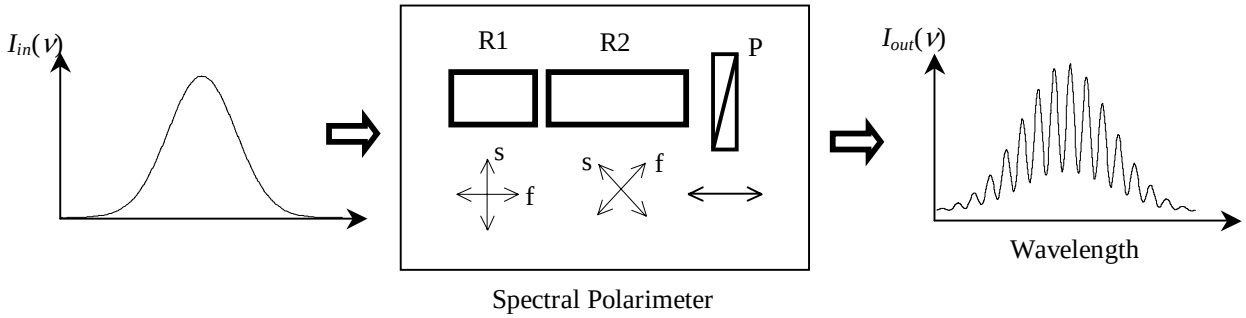

Figure 2. Schematic of the spectral polarimeter

where $\Im$ stands for the operator of the Fourier transform, x denotes the optical path length difference and $\Delta n = n_s - n_f$ is the birefringence of the retarder. As seen in Equation (6), the seven components of the signal have information about each components of spectral Stokes parameters and are satisfactorily resolved from one another in the optical path length difference domain, centered at $x = 0, \pm\Delta nL_2, \pm\Delta n(L_2-L_1), \pm\Delta n(L_2+L_1)$.
Inverse Fourier Transform of the first, second and fourth terms of Equation (6), which correspond to the central, second and first peaks on the optical path length differnce domain, respectively, gives

$$\frac{1}{2}S_0(\nu) \tag{7.a}$$

$$\frac{1}{4}S_1(\nu)e^{i\varphi_2(\nu)} \tag{7.b}$$

$$\frac{1}{8}[S_2(\nu) - iS_3(\nu)]e^{i(\varphi_2(\nu)-\varphi_1(\nu))}. \tag{7.c}$$

Since phase retardations, $\varphi_1(\nu)$ and $\varphi_2(\nu)$ are independent of the incident light and determined only by lengths and birefringence of the two retarders, they can be calibrated by use of the incident light with a known polarization state. As a result, we can obtain the unknown polarization state of incident light with single intensity measurement using a spectral polarimeter.
A fiber optic spectral polarimeter is an all-fiber based instrument with the characteristic of a spectral polarimeter. Figure 3 shows the diagram of the fiber optic spectral polarimeter. Light emitted by an optical semiconductor amplifier (AFC technologies, λ=1.31 μm, FWHM=62 nm) is delivered with a single mode fiber (SMF-28) and coupled to a fiber optic spectral polarimeter. A polarizer/retarder module is used to set the polarization state of input light. Polarization maintaining fibers (PM fiber, Panda, $L_B=\lambda/\Delta n$=2.8 mm) spliced at 45° with respec to each other are used as a retarder system (R1 and R2) in the fiber optic spectral polarimeter. PM fiber is a birefringent fiber, i.e., has two orthogonal axes with different refractive indices due to internal stress structures. A polarizer module is oriented so that its transmission axis is parallel to the fast axis of the first PM fiber. The lengths of two PM fibers are chosen as 1 *m* and 2 *m*, respectively, so that the seven components of the spectral polarimetric output signal are displaced by the same interval in the optical path length difference domain. Output signal from the fiber optic spectral polarimeter is coupled into a fiber Fabry-Perot tunable filter (FFT-TF, Micron Optics Inc., FSR=10.2 THz (58 nm), Bandwidth=14.4 GHz (0.08 nm), Tuning voltage/FSR=12 V, Maximum Tuning Voltage=70 V) in line with a photoreceiver (New Focus, 2011-FC). The FFP-TF is an all-fiber, plane Fabry-Perot interferometer with a single-mode optical fiber waveguide segment and an air gap between two highly reflective multilayer mirrors deposited directly onto optical fibers. A Fabry-Perot interferometer acts as a band-pass filter depending on the distance between two mirrors [1]. By application of a variable drive voltage to a FFP-TF, nanometer axial movement of the mirrors is achieved and wavelength tuning is possible.
The use of the FFP-TF for wavelength tuning instead of a grating based spectrometer makes the system all-fiber based that can be packaged in compact space.

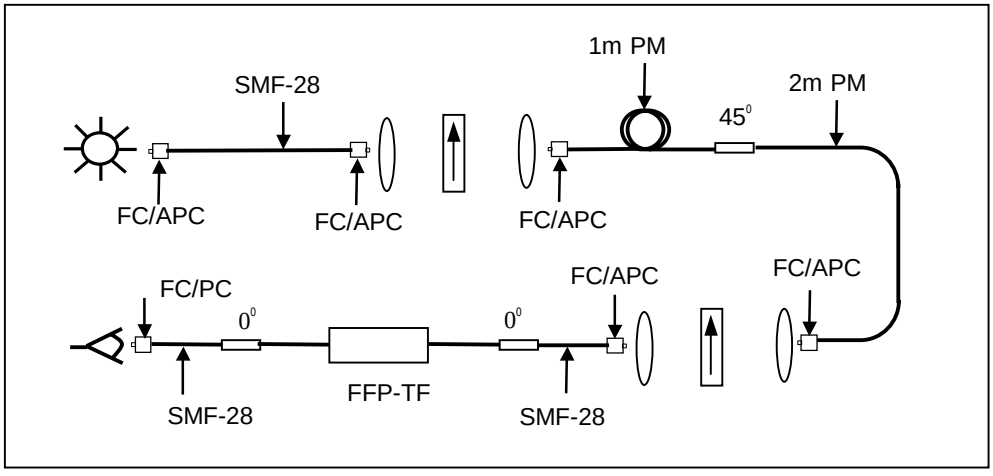

Figure 3. Fiber Optic Spectral Polarimeter

4. RESULTS AND DISCUSSION

Figures 4-6 show the results of the measurements of the polarization state of the input light with known polarization state. For these measurements, we used a band pass filter (Laser Line Filter, 1310NB40, $\Delta\lambda$=40 nm (6.99 THz), Omega Optical Inc.) to reduce the bandwidth of the input light and the measurements were performed over about 1 FSR. Estimation of the phase retardations, $\varphi_1(v)$ and $\varphi_2(v)$, is required to reconstruct the spectrally resolved Stokes parameters (Equation 7). To calibrate $\varphi_2(v)$, inverse Fourier transform of the second peak in the electrical frequency (optical path length difference) domain was performed for a horizontally polarized input light and its argument was fitted using a least squares fitting algorithm up to the group velocity dispersion term. Likewise, $\varphi_2(v)$- $\varphi_1(v)$ was calibrated using the first peak of a linearly polarized input light at 45° with respect to the optical table.

Figure 4(a) and (b) show the measured output spectrum and its Fourier transform for a horizontally polarized input light. One encouraging result is the depth of modulation in the signal is big enough to make the fiber optic spectral polarimeter feasible. Also, the Fourier transform of the measured signal shows the only central and second peaks corresponding to S_0 and S_1, respectively as expected. Inverse Fourier transforms of each peak provide the spectral resolved the Stokes parameters and the results are presented in Figure 4(c)-(f). The results show the large S_1, and small S_2 and S_3 over whole frequency regions as expected. However, unexpected small amplitude oscillation appears in the reconstructed Sotkes parameters and it is not certain whether it is from a system itself such as polarization mode dispersion in the PM fiber, or numerical error from analyzing process at this point. We expect quantifying the dispersion of a retarder system may help to remove this oscillation.

Figure 5(a) and (b) show the measured output spectrum and its Fourier transform for a linearly polarized light at 45° to the optical table. It is evident that the output spectrum is modulated differently with different polarization state of input light and the Fourier transform of the spectrum gives only central, first and third components corresponding to S_0 and S_{23} as expected. However, a small energy distribution is observed at the region around the location of the second component corresponding to S_1. The feature may be due to an overlap of first and third components or a real S_1 component due to slight misalignment of an input polarizer module. To be sure, we need to build another retarder system with longer PM fibers. The reconstructed Stokes parameters are presented in Figure 5(c)-(f) and show large S_2, and small S_1 and S_3.

Figure 6(a) and (b) show the measured output spectrum and its Fourier transform for a circularly polarized input light. The measured signal is observed to modulate with same frequency as the case of linearly polarized input light at 45° since the inverse Fourier transform of the first peak includes the S_2 and S_3 components together in real and imaginary part, respectively. The reconstructed Stokes parameters are presented in Figure 6(c)-(f).

5. CONCLUSIONS

The fiber optic spectral polarimeter, the instrument that allows the measurement of spectral dependent Stokes parameters was constructed and tested. The experimental results for the input light with known polarization states verified the performance of the fiber optic spectral polarimeter.

The fiber optic spectral polarimeter itself is the novel technique to allow measurements of the spectral-dependent polarization state faster than existing techniques. Moreover, it can be incorporated into a tomographic imaging system such as a conventional microscopy system. This system will provide measurements that will allow an understanding of depolarization process of light passing through biological materials for diagnostic imaging. A recent study has indicated that polarized light may be useful in the discrimination between the normal and malignant tumor samples [18,19]. Therefore, the proposed imaging technique with a fiber optic spectral polarimeter can be used for the early cancer detection.

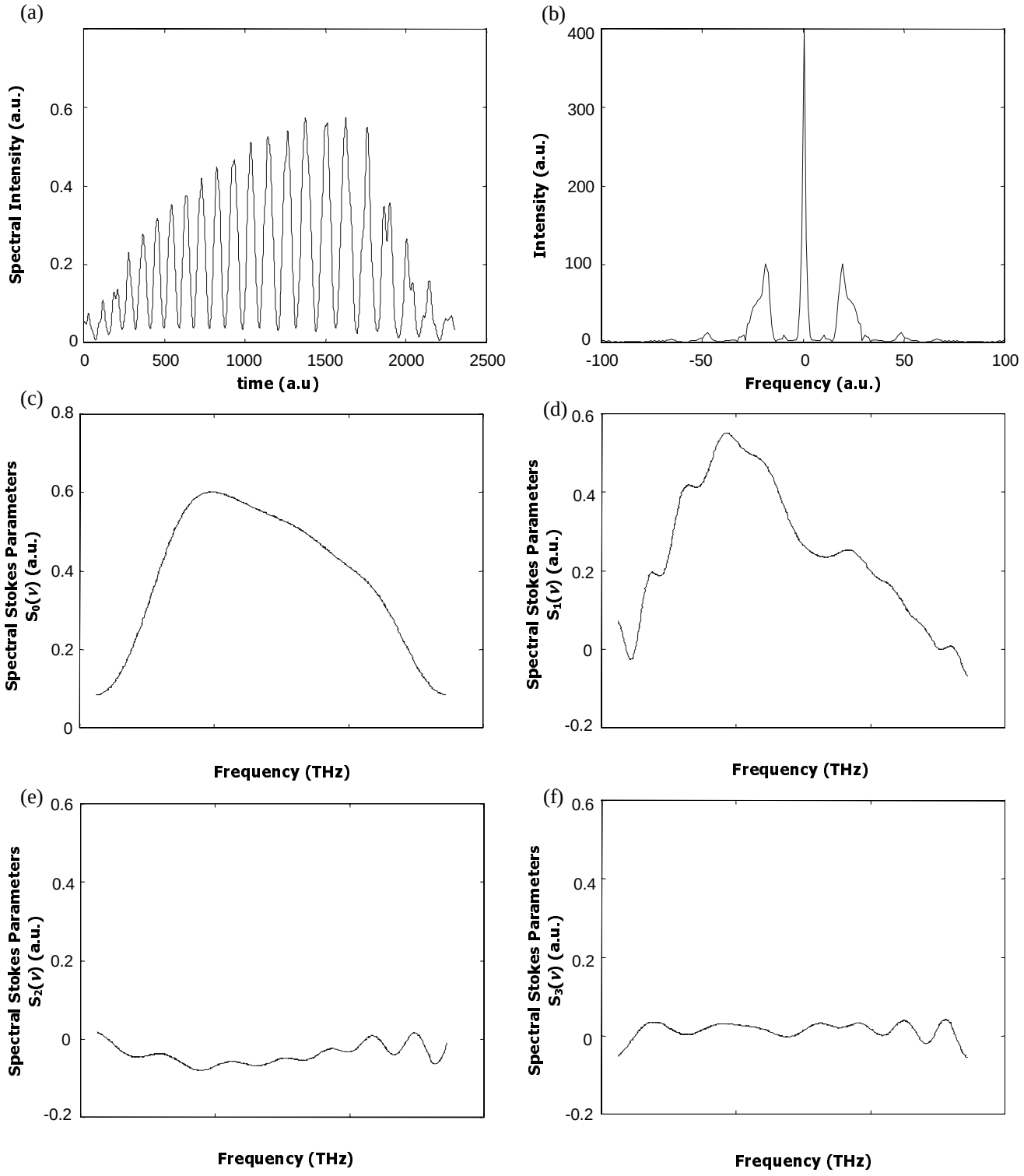

Figure 4. Horizontally Polarized Light: (a) Measured Spectral Intensity. (b) Magnitude of FFT of (a). (c) Reconstructed Spectral Stokes Parameter, $S_0(\nu)$. (d) Reconstructed Spectral Stokes Parameter, $S_1(\nu)$. (e) Reconstructed Spectral Stokes Parameter, $S_2(\nu)$. (f) Reconstructed Spectral Stokes Parameter, $S_2(\nu)$.

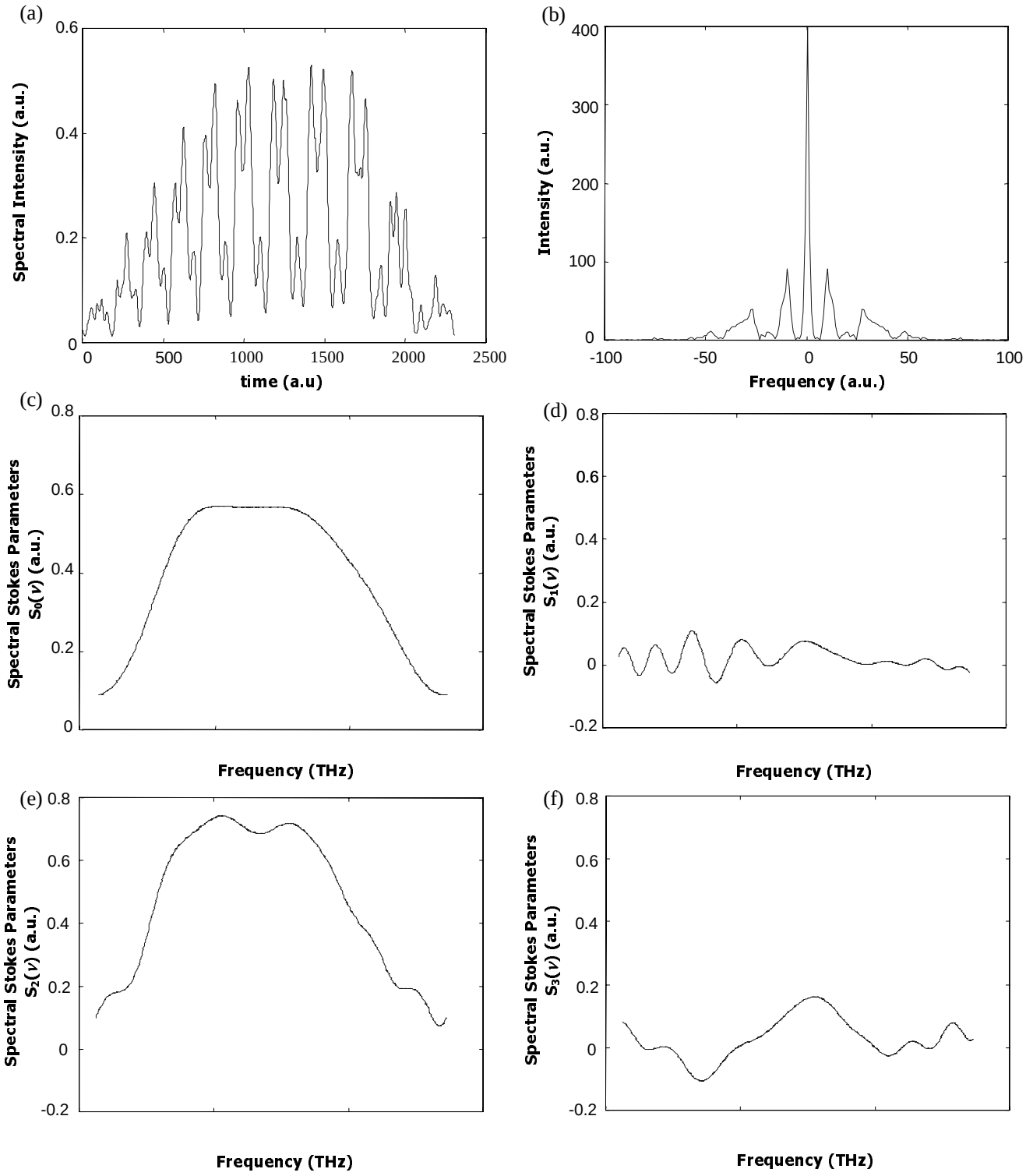

Figure 5. Linearly Polarized Light at 45°: (a) Measured Spectral Intensity. (b) Magnitude of FFT of (a). (c) Reconstructed Spectral Stokes Parameter, $S_0(\nu)$. (d) Reconstructed Spectral Stokes Parameter, $S_1(\nu)$. (e) Reconstructed Spectral Stokes Parameter, $S_2(\nu)$. (f) Reconstructed Spectral Stokes Parameter, $S_2(\nu)$.

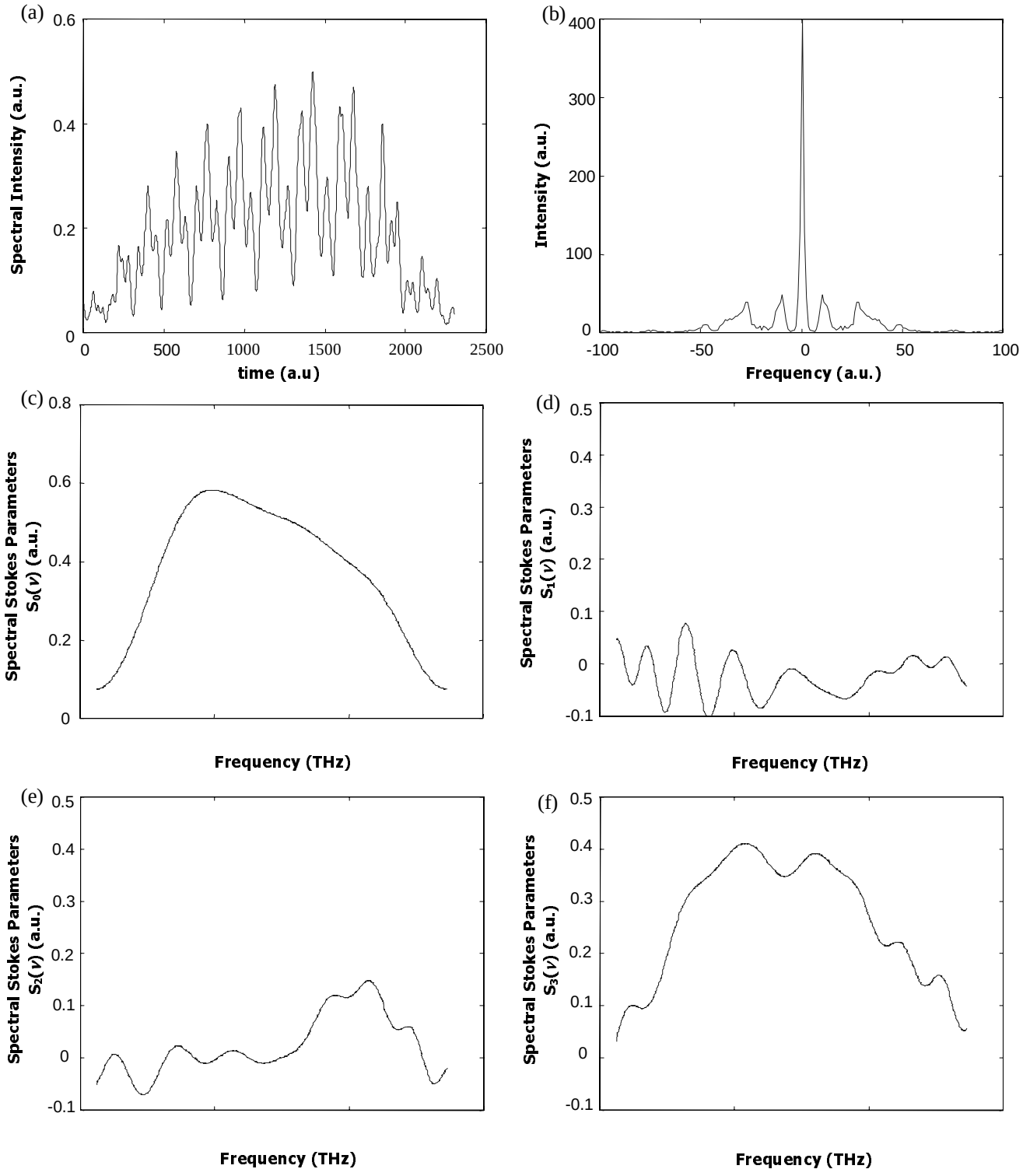

Figure 6. Circularly Polarized Light: (a) Measured Spectral Intensity. (b) Magnitude of FFT of (a). (c) Reconstructed Spectral Stokes Parameter, $S_0(\nu)$. (d) Reconstructed Spectral Stokes Parameter, $S_1(\nu)$. (e) Reconstructed Spectral Stokes Parameter, $S_2(\nu)$. (f) Reconstructed Spectral Stokes Parameter, $S_2(\nu)$.

REFERENCES

1. J. M. Schmitt, A. H. Gandjbakhche, and R. F. Bonner, "Use of polarized light to discriminate short-path photons in a multiply scattering medium", Appl. Opt., **31**, 6535 (1992)
2. S. P. Morgan, M. P. Khong, and M. G. Somekh, "Effects of polarization state and scatterer concentration on optical imaging through scattering media", Appl. Opt., **36**, 1560 (1997)
3. V. Sankaran, K. Schönenberger, J. T. Wlash Jr., and D. J. Maitland, "Polarization discrimination of coherently propagating light in turbid media", Appl. Opt., **38**, 4252 (1999)
4. P. Gleyzes, A. C. Boccara, and H. Saint-Jalmes, "Multichannel Nomarski microscope with polarization modulation: performance and applications", Opt. Lett. **22**, 1529 (1997)
5. S. P. Schilders, X. S. Gan, and M. Gu, "Resolution improvement in microscopic imaging through turbid media based on differential polarization gating", App. Opt. **37**, 4300 (1998)
6. K. Schönenberger, B. W. Colston Jr., D. J. Maitland, L. B. Silva, and M. J. Everett, "Mapping of birefringence and thermal damage in tissue by use of polarization-sensitive optical coherence tomography", Appl. Opt., **37**, 6026 (1998)
7. J. F. de Boer, S. M. Srinivas, A. Malekafzli, Z. Chen, J. S. Nelson, "Imaging thermally damaged tissue by polarization sensitive optical coherence tomography", Opt. Exp., **3**, 212 (1998)
8. M. G. Ducros, J. F. de Boer, H. Huang, L. C. Chao, Z. Chen, J. S. Nelson, T. E. Milner, and H. G. Rylander, III, "Polarization Sensitive Optical Coherence Tomography of the Rabbit Eye", IEEE Journal of Selected Topics in Quantum Electronics, **5**, 1159 (1999)
9. J. M. Schmitt and S. H. Xiang, "Cross-polarized backscatter in optical coherence tomography of biological tissue", Opt. Lett. **23**, 1060 (1998)
10. S. Jiao, G. Yao, and "L. V. Wang, "Depth-resolved two-dimenstional vectors of backscattered light and Mueller matrices of biological tissue measured with optical coherence tomography", App. Opt. **39**, 6318 (2000)
11. S. P. Morgan and M. E. Rdigway, "Polarization properties of light backscattered from a two layer scattering medium", Opt. Exp. **7**, 395 (2000)
12. S. G. Demos, H. B. Radousky and R. R. Alfano, "Deep subsurface imaging in tissue using spectral and polarization filterng", Opt. Exp., **7**, 23 (2000)
13. E. Hecht, *Optics*, Addison-Wesley, 1987 (2nd Edition)
14. W. A. Shurcliff, Polarization of Light; Production and Use, Cambridge, 1962
15. K. Oka and T. Kato, "Spectroscopic polarimetry with a channeled spectrum", Opt. Lett. **24**, 1475 (1999)
16. C.T. Kelley, *Iterative Methods for Linear and Nonlinear Equations*, Fontiers in Applied Mathematics Vol.16, SIAM, 1995
17. J. W. Goodman, Statistical Optics, John Wiley & Sons, 1985
18. A. Pradhan, R. N. Panda, M. S. Nair, B. V. Laxmi, A. Agarwal and A. Rastogi, "Fluorescence study of normal, benign, and malignant human breast tissues", Proc. SPIE **3917**, 240 (2000)
19. M. Rajadhyaksha, G. Menaker, and S. Gonzalez, "Confocal microscopy of excised human skin using acetic acid and crossed polarization: rapid detection of non-melanoma skin", Proc. SPIE **3907**, 84 (2000)